PAPER • OPEN ACCESS

Strain relief and shape oscillations in site-controlled coherent SiGe islands

To cite this article: N Hrauda *et al* 2013 *Nanotechnology* **24** 335707

View the article online for updates and enhancements.

Strain relief and shape oscillations in site-controlled coherent SiGe islands

N Hrauda[1], J J Zhang[1,2], H Groiss[1,3], T Etzelstorfer[1], V Holý[4], G Bauer[1], C Deiter[5], O H Seeck[5] and J Stangl[1]

[1] Institute for Semiconductor Physics, Johannes Kepler University Linz, Altenbergerstrasse 69, A-4040 Linz, Austria
[2] Centre for Quantum Computation and Communication Technology, School of Physics, The University of New South Wales, Sydney NSW 2052, Australia
[3] Laboratory for Electron Microscopy, Karlsruhe Institute of Technology, PO Box 3640, D-76021 Karlsruhe, Germany
[4] Faculty of Mathematics and Physics, Charles University Prague, Ke Karlovu 5, Praha, 12116, Czech Republic
[5] Deutsches Elektronen-Synchrotron DESY, Notkestraße 85, D-22607 Hamburg, Germany

E-mail: nina.hrauda@jku.at, Jianjun.Zhang@unsw.edu.au and heiko.groiss@lem.uni-karlsruhe.de

Abstract
Strain engineering and the crystalline quality of semiconductor nanostructures are important issues for electronic and optoelectronic devices. We report on defect-free SiGe island arrays resulting from Ge coverages of up to 38 monolayers grown on prepatterned Si(001) substrates. This represents a significant expansion of the parameter space known for the growth of perfect island arrays. A cyclic development of the Ge content and island shape was observed while increasing the Ge coverage. Synchrotron-based x-ray diffraction experiments and finite element method calculations allow us to study the strain behavior of such islands in great detail. In contrast to the oscillatory changes of island shape and average Ge content, the overall strain behavior of these islands exhibits a clear monotonic trend of progressive strain relaxation with increasing Ge coverage.

S Online supplementary data available from stacks.iop.org/Nano/24/335707/mmedia

(Some figures may appear in colour only in the online journal)

1. Introduction

Silicon and germanium have been key materials for semiconductor physics and technology since the very beginning. When it comes to strain engineering they are excellent to be combined when designing devices—they have the same crystal structure, but lattice parameters that differ by an amount of 4.2%. This mismatch leads to strain in the resulting hetero-epitaxial structure, which can be utilized to modify the band structure in bulk [1] as well as in nanostructured materials [2–4]. For instance,

the exact transition energies and optical transition matrix elements depend sensitively on the particular distributions of chemical species as well as strain inside nanoscale objects [5–8]. A serious issue, however, is defect formation during growth caused by the very strain one initially wants to employ to optimize device properties [9, 10]. This is especially the case for the two-dimensional SiGe stressor layers that are commonly used for fabrication. Such defects, in particular misfit dislocations, can hamper or even destroy the functionality of the device.

Thus a balance needs to be found between introducing maximum strain and avoiding defects in the crystal structure. With an appropriate design, strain can be exploited during growth to drive a two-dimensional (2D) to three-dimensional (3D) morphological transition, which is used to fabricate

self-assembled SiGe nanoislands in the Stranski–Krastanov growth mode [11–15]. Defect-free SiGe islands offer various possibilities in silicon-based applications that profit from strain engineering. Either the strain inside SiGe islands and in a Si cap on top of them are used directly [16–21], or it can be further enhanced by adding external stressors [4]. The growth processes during deposition of a few—in most cases up to around ten—monolayers (ML) of Ge on Si(001) have been studied in detail [11, 22–26].

Our results show that the parameter space for the formation of defect-free islands is actually larger than previously thought. We show that considerably more Ge can be deposited on Si(001) without the formation of misfit dislocations and that ultra-steep islands evolve. Strain relaxation is revealed to be the main driving force of a rather complex evolution of island shape and Ge distribution.

So far, the following commonly accepted sequence when increasing the Ge coverage was established (for high growth temperatures above about 550°): first, the formation of a Ge wetting layer with a certain thickness (approximately 3–4 ML Ge), then pre-pyramids [27] and hut clusters evolve [12], followed by pyramids [28], then domes [29, 22] and barns [30]. The aspect ratio of the islands is constantly increasing during this process [31, 32]. If the deposition of Ge is continued further, so-called superdomes form [33, 32, 34]. These islands develop dislocations to plastically relax the strain built up during growth, which is well documented in the case of SiGe islands grown on flat substrates [32]. Therefore, until recently it was believed that barns represent the upper size limit for defect-free SiGe islands. Only for high growth temperatures of around 900 °C, where Si–Ge intermixing is very prominent and reduces the effective lattice mismatch, could larger defect-free islands be realized [35].

In the case of Ge growth on patterned Si substrates this behavior is markedly different. While at first the island shape evolution is the same as known from flat substrates [24], it was found that both the island shape and average Ge content undergo a cyclic evolution if the Ge deposition is increased beyond a certain amount of Ge, depending on the pattern configuration [36]. In this case defect formation, which is the cause for shape changes to superdomes in other studies [33], can be delayed. Instead, barn-shaped islands at some point change back into domes by increasing the diameter and incorporating Si from the surrounding area. During this transition the island height stays approximately constant while the average Ge content decreases. Continuing the deposition of Ge, these domes then evolve back into barns by building up in height. In such a way, the island volume increases by in turn, extending either the height or diameter. The islands of such a growth series can be denominated as P_1–D_1–B_1–D_2–B_2–D_3 (P = pyramid, D = dome, B = barn; the numbers denote the growth cycle).

In this paper we address the following questions: how much Ge can we deposit on a pit-patterned substrate before the onset of dislocations? Does shape oscillation continue? What is the strain state of such islands?

The boundary conditions of the presented study are the following: as substrate, pit-patterned Si(001) substrates were used (quadratic arrangement of pits with 500 nm periodicity); the amount of deposited Ge ranges from 15 to 38 monolayers (ML); the substrate temperature during Ge deposition was 720 °C.

Our investigations are based on atomic force microscopy (AFM), transmission electron microscopy (TEM) and synchrotron-based high resolution x-ray diffraction (XRD). To obtain additional information on the Ge distribution a tomographic method based on selective etching in combination with AFM scans was used [37, 38]. The etching process stops at alloys with low Ge ratios of 5%–10% [39], which leads to a certain error, especially at the island base and the regions below. We therefore rely on a combination of the results obtained by this technique with experimental XRD data to refine the Ge distributions for strain calculations. The strain fields are obtained by detailed finite element method (FEM) model calculations.

It was found that aspect ratio, shape and average Ge content of the SiGe islands continue their oscillating behavior with further Ge deposition, forming steeper barns or steep cupolas, respectively. However, the analysis presented in this paper shows that the development of the island strain state follows a strictly monotonic trend towards enhanced strain relaxation with ongoing Ge deposition, despite the changes in Ge content and island shape.

2. Sample growth and experimental methods

Si(001) substrate pieces of 9×9 mm^2 size were patterned by holographic lithography and reactive ion etching (RIE), resulting in a regular pattern of approximately circular pits with 500 nm lateral period. Both the depth of the pattern holes as well as the Si coverage for the buffer layer were chosen with respect to the planned amount of Ge to be deposited—e.g. for samples with high Ge coverages the diameter and depth of the pattern hole was increased (see table S1 in the supplementary data available at stacks.iop. org/Nano/24/335707/mmedia). All samples were grown by solid-source MBE using a Riber SIVA 45 system. Si-buffer layer thicknesses ranged from 36 to 55 nm. The growth temperature during Si-buffer deposition was ramped up from 450 to 550 °C. Ge was deposited at 720 °C and a growth rate of 0.03 Å s^{-1}. The amount of deposited Ge was 15, 19, 26, 30 and 38 ML Ge, respectively.

The surface morphology of the samples was studied using a Digital Instruments Dimension 3100 AFM operating in tapping mode. Furthermore, surface orientation maps (SOM) are provided (see insets of figure 1) where 'intensity peaks' indicate an increased occurrence of surfaces with a certain azimuth and inclination angle. One issue of this technique is that only surface inclination angles up to about 60° can be detected (with conventional AFM techniques) due to the geometry of the AFM tip. Thus the steepest facets of the islands resulting from 30 and 38 ML Ge are not visible in AFM scans shown here, but were found by TEM.

TEM investigations were performed with a JEOL JEM-2011 FasTEM at 200 keV equipped with a CCD camera. For an enhanced mass–thickness contrast, the samples were
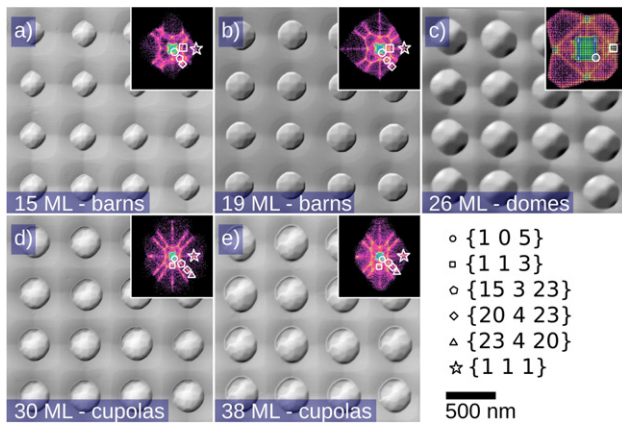
Figure 1. AFM images and surface orientation maps (insets) of SiGe islands grown on 500 nm pit patterns. After barn-shaped islands B_2 ((a), (b)), domes of the third growth cycle D_3 evolve (c), followed by steep cupola-shaped islands C_3 ((d), (e)) for the highest amounts of deposited Ge. The steepest facets of the cupolas are not visible in the AFM data due to the geometry of the AFM tip, but were confirmed by TEM investigations.

investigated near a two-beam condition (TBC) for the forbidden (002) diffraction spot to avoid strong diffraction contrast. Crystal defects, which locally destroy the crystal symmetry and thus influence the diffraction spot selection rules, would lead to a strong contrast that could be detected easily. Bright-field images recorded at this TBC exhibit a strong mass–thickness contrast, highlighting Si–Ge gradients (Ge appears darker) and interfaces.

XRD experiments were carried out at the high-resolution diffraction beamline P08 at the Petra III synchrotron in Hamburg [40]. An energy of 8.048 keV, corresponding to a wavelength of Cu Kα ($\lambda = 1.5406$ Å) was used. Reciprocal space maps (RSM) around the symmetric (004) and the asymmetric (224) Bragg peak were recorded using a MYTHEN 1D position sensitive detector [41]. The maps (see figure 2) include both the sharp and intense Si bulk signal as well as the SiGe island signal, which, due to the small scattering volume provided by the islands, has a rather low intensity. The diffracted intensity from Si with the smaller lattice constant is situated at higher reciprocal space coordinates Q_x and Q_z (corresponding to the in-plane [1 1 0] direction and the surface normal [0 0 1], respectively) than that of pure Ge or a SiGe alloy. The Ge content within the islands is not constant or even continuous but has a certain concentration distribution that leads to a variation of the lattice constant within the SiGe islands. Combined with the shape and size, this results in a characteristic distribution of the scattered intensities in reciprocal space.

Increased intensities directly below the Si bulk peak or a separated signal close to the Si bulk position are a hint that the SiGe-alloyed regions below the island are quite extended, see the RSMs shown in figures 2(e) and (f) of the 26 ML sample (domes) and figures 2(i) and (j) of a sample containing steep cupolas (38 ML Ge). The Ge content in those regions is usually too low to be captured by selective etching experiments. Still, those areas have a significant influence

on the relaxation state of the SiGe island and need to be taken into account when performing strain calculations. We observe streaks in the vicinity of the Si substrate signal that occur due to the shallow pit facets surrounding the islands (e.g. figure 2(c)). The lateral pit-pattern periodicity of 500 nm leads to fine intensity oscillations around the Si bulk peak and the SiGe island signal, as seen in figure S2 in the supplementary material (available at stacks.iop.org/Nano/24/335707/mmedia).

The calculation of the strain fields was carried out based on the Finite Element Method using the commercial *COMSOL Multiphysics* package [42]. XRD simulations for comparison with the experimental data were performed using a Fortran code written by Holý, based on kinematical scattering theory [43, 44]. This code uses the displacement fields generated by the FEM simulations as input.

To eliminate the influence of island shape on the results, we used the exact shape obtained from AFM and TEM data. The XRD results are actually not sensitive to minor changes in individual facet areas, but it is important to correctly describe the island's overall shape and aspect ratio. The Ge distribution is modeled by mathematical functions with a few free parameters, which are fitted to obtain a good match between experiment and simulations. Slight changes in the distribution functions can be compensated by slight changes in the free parameters. Overall, the approach is sensitive to changes of about 2–3 at.% in the local Ge content. For more details on creating the island FEM model, establishing the Ge distribution and performing the x-ray simulations and the refinement process, see the supplementary data (available at stacks.iop.org/Nano/24/335707/mmedia).

3. Discussion

3.1. Evolution of the pit morphology

For the correct calculation of the strain fields in a SiGe island it is of utmost importance to have a look at the processes that take place during island nucleation. For this purpose we performed AFM investigations on three additional samples with the same pattern properties, directly after Si-buffer deposition and after 3.5 and 6 ML Ge, respectively.

Figure 3 depicts the evolution of the surface morphology at a pit location, for increasing amounts of deposited Ge: it includes AFM scans of samples directly after pattern etching, Si-buffer growth, at the onset of island nucleation and data on samples containing SiGe islands. The dark gray line represents a scan of the original pattern hole after RIE. The Si buffer (blue line) deposited on the substrate partially fills the pits, transforming it into an inverted dome shape. After 3.5 ML Ge (green line), the initially deep pit has flattened out and is now defined by {1 0 5} facets. The deposition of the first few MLs of Ge leads to a mobilization of Si atoms at the surface, resulting in a material transport from the regions between the pits into the pits. Hence the pit depth is reduced and its sidewalls become shallower. The bottom of the pits is filled with a dilute SiGe alloy due to the codiffusion of Si and Ge at the growing surface [45, 46].
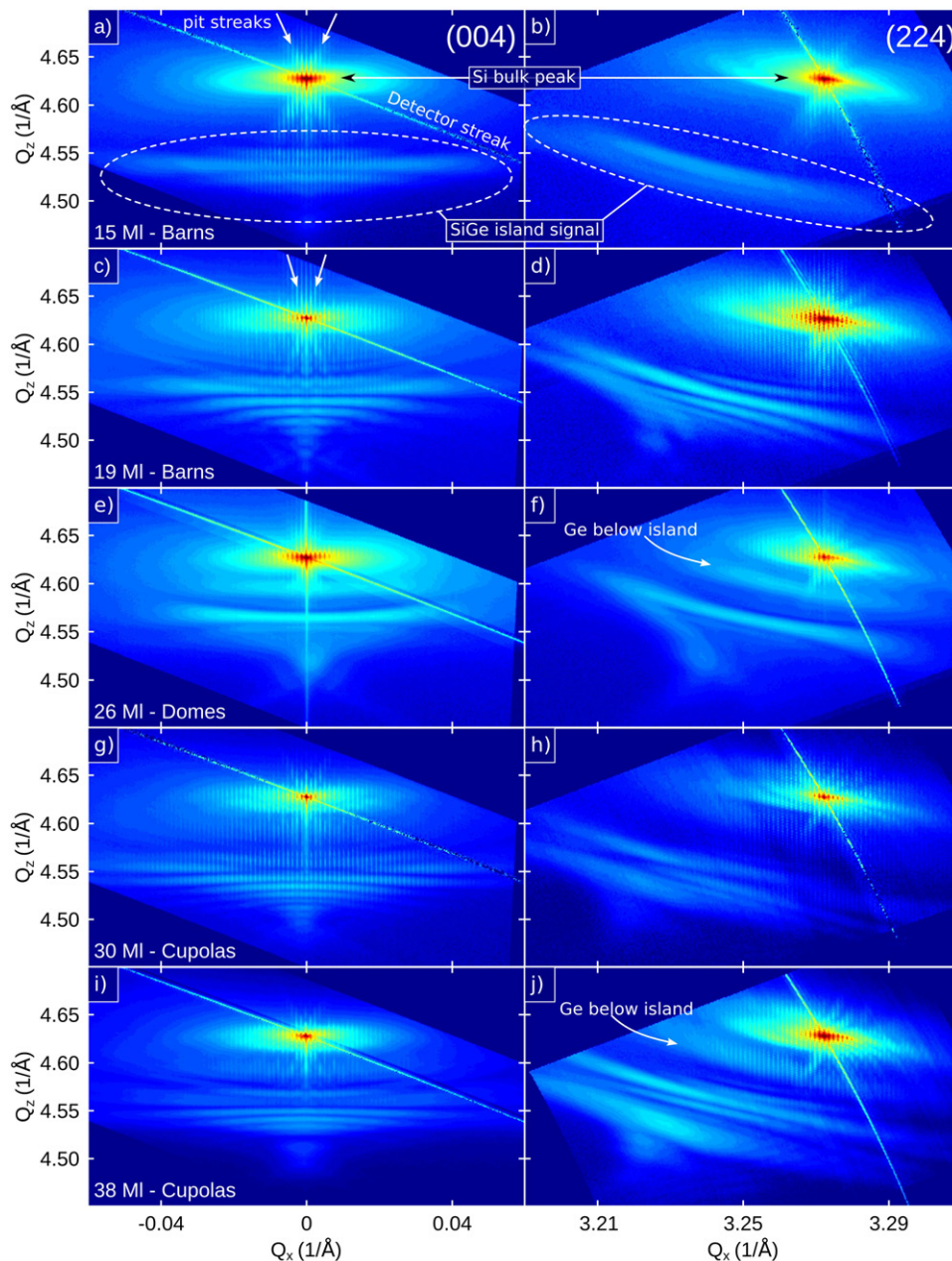
Figure 2. (004) and (224) RSMs of the five samples with a 500 nm pattern period and increasing amount of Ge deposition (15–38 ML Ge).

The degree of intermixing and the dimension of the affected regions vary strongly with growth parameters and the geometry of the pattern, for example the pattern period and the size of the pattern holes. Pyramid-shaped islands are observed after 6 ML Ge (orange), domes after 9 ML (orange) and barn-shaped island after 15 ML Ge deposition. The purple profile in figure 3 represents a cupola-shaped island found at Ge coverages of 30 ML.

3.2. SiGe islands from high Ge coverages

For the samples discussed in the following we are already well beyond the first growth cycle (P_1–D_1–B_1–D_2) for this specific pattern [36]. These island samples with coverages ranging from 15 to 38 ML Ge can be assigned to the

second and third cycle (B_2–D_3–SC_3, with SC = steep cupola). The AFM images and surface orientation maps (SOM) are shown in figure 1. The two samples with the highest Ge coverage featuring cupola-type [35] islands (30 and 38 ML Ge, see figures 1(d) and (e)) display ultra-steep surfaces with inclination angles up to 80° with respect to the (001) surface, however, those facets cannot be assessed by conventional AFM techniques. Detailed descriptions of the island shapes along with the characteristic facet sets can be found in the supplementary data (available at stacks.iop.org/Nano/24/335707/mmedia), a graphical representation is given in figure 7. The islands resulting from a Ge coverage of 15 and 19 ML both exhibit a barn geometry (see figures 1(a) and (b)) with aspect ratios slightly below 0.3. These two samples represent barns of the second growth cycle (B_2). The
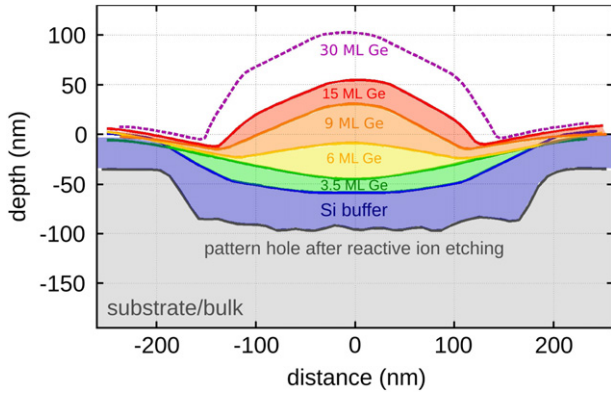
Figure 3. Linescans of AFM images from a representative pit region in samples obtained by depositing increasing amounts of Ge on a prepatterned Si(001) surface. The dark gray line represents the pattern hole directly after RIE, which, to eliminate roughness and impurity related effects, is covered with Si buffer (blue profile), thereby evolving into a multifaceted pit. When the deposition of Ge is started the pit depth is decreased and defined by shallower facets (green). Subsequently, pyramid-shaped islands (yellow) start to develop, which at some point change into dome-shaped islands (orange) and subsequently to barns (red). The dashed purple line represents a further island type that occurs at high Ge coverages after several shape transformations, the so-called steep cupolas.

indicates the onset of increased Si incorporation preceding the transformation from barns back to domes [36]. 2D maps of the strain distributions are shown in figure 4. The average in-plane and out-of-plane strain values for the 15 ML sample are −0.61% and 0.49%, respectively. The values for the larger 19 ML sample are lower, with −0.49% in-plane and 0.39% out-of-plane.

The sample obtained by depositing 26 ML Ge displays an increase of its diameter to 360 nm, while the height is reduced to 74 nm (figure 1(d)) and thereby marks the onset of a third growth cycle (D$_3$). The resulting low aspect ratio of 0.2 is typical for domes. Both the mass contrast seen in TEM images shown in figures 5(a) and (b), as well as the etching profile in figure 5(c), reveal extensive amounts of Ge situated below the island. The Ge distribution as determined by XRD and FEM simulations features an inner core of 25%, an intermediate section of 22% and a shell with a maximum content of 34%, which is laterally decreasing by 5% (see figure 4(g)). The average Ge percentage for the pitfill and island section together is 26%. The average in-plane and out-of-plane strain values decrease to values of −0.46% and 0.36%, respectively, continuing the relaxation trend despite the dramatic shape change.

Regarding their exceptional geometries (see figure 6), the SiGe islands of the last two samples with 30 and 38 ML Ge can be referred to as steep cupolas. TEM investigations on the 38 ML sample revealed the existence of a ultra-steep facet or surface set that has not been observed before. Images of TEM-lamellae cut parallel to the [1 1 0] direction show these ultra-steep surfaces at the island base (see figures 6(a) and (c)).
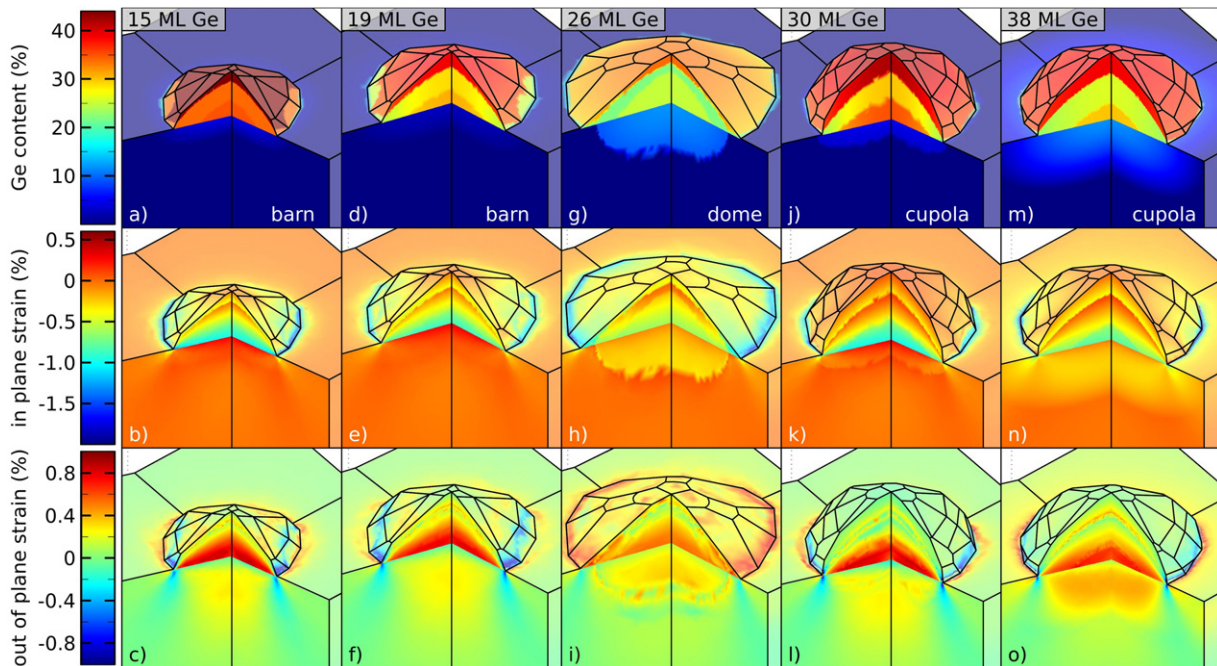
difference between the 15 and 19 ML islands is an increase in island diameter from 230 to 280 nm and a slight increase in height from 64 to 77 nm. This results in a lower aspect ratio for the 19 ML sample. The average Ge content is 35.6% for the 15 ML and 29.7% for the 19 ML sample, which

Figure 4. Results of the FEM simulations for samples resulting from 15 to 38 ML of Ge. Shown are the Ge content, the in-plane strain $\varepsilon_\parallel$ and the out-of-plane strain ε_{zz} displayed on the surface of the model as well as along two cuts through the center of the model block (*x* and *y* direction). Ge was applied in the areas below the pit if certain features of the Si peak or distinct SiGe signals close to the Si bulk peak indicated its presence.
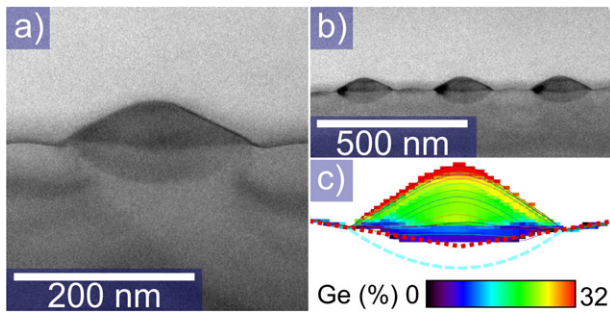
Figure 5. TEM images ((a), (b)) of the domes obtained by the deposition of 26 ML Ge and the corresponding Ge profile as a result of AFM-based nanotomography (c). The TEM images were taken with the sample slightly disoriented from the zone axis to observe the mass contrast (Ge appears darker). Both TEM and etch profiles show that a region of low Ge content extends down below the island (light blue dashed line), deeper than the shallow {1 0 8} surfaces would account for (red dotted line).

Taking the {1 1 1} facet as reference, an inclination angle of 80° (±2) was determined. This corresponds to a surface with the Miller indices {4 4 1} (inclination angle of 79.97°). This surface probably consists of microfacets, as the {4 4 1} facet was not reported as a stable one for the SiGe system so far [47, 48]. A plane-view TEM image of the 38 ML sample is shown in figure 6(e). Remarkable is the regular and symmetric pattern of the strain contrast throughout the island, which is a clear indication for the absence of dislocations.

The model geometry of the 30 ML sample is based on a diameter of 280 nm and a height of 109 nm, obtained from TEM and AFM data, resulting in an aspect ratio of 0.39. The Ge profile for this sample is shown in figure 4(j) and the average Ge content is 33%. The 38 ML sample has a slightly lower height compared to the previous one at 105 nm, but an increased diameter of 300 nm and an aspect ratio of 0.35. Its average Ge content is significantly lower at 30%. The average

strain values within the island are the same for those two samples with −0.35% in-plane and 0.29% out-of-plane.

The combination of methods consistently shows that on pit-patterned substrates defect-free, i.e. coherent islands can be grown with substantially higher volumes than previously reported [25]. Figure 7 summarizes the evolution of the main island shapes in pits starting with pyramids and ending with the steep cupolas. During the sequence, islands grow alternately in diameter and height. Depositing 40 MLs of Ge resulted in the formation of defects within the islands.

To obtain the general trends, several key parameters obtained by our simulations in dependence of the Ge coverage (given in monolayers) have been extracted from the data and are summarized in figure 8. With increasing coverage, the island volumes increase steadily and reach values well above 4×10^6 nm^3, considerably larger than what was thought so far the limit for growth on pit-patterned substrates [49]. We suggest that the reason for the delay in dislocation formation is the increased relaxation due to regions of low Ge content below the islands, so that they form on an already slightly relaxed 'support' [25, 50].

The changes in aspect ratio upon transition from one shape to another coincide with changes in the Ge distribution, which manifest themselves also in the average Ge content. For instance, the decrease of the aspect ratio when the island shape transforms from a barn back to a dome is accompanied by a reduction of the Ge content due to increased intermixing with silicon. Figure 8(b) documents the 'oscillating' behavior of the average Ge content in dependence of shape changes. One might expect that the island's relaxation and hence average strain reflect this oscillating Ge content. However, the averaged strain values show a clear monotonic trend over the complete sample series, as seen in figure 8(c) (dark blue line). Both in-plane and out-of-plane strain values decrease with increasing Ge coverage, the system exhibits an enhanced relaxation of the islands with ongoing Ge deposition. This is
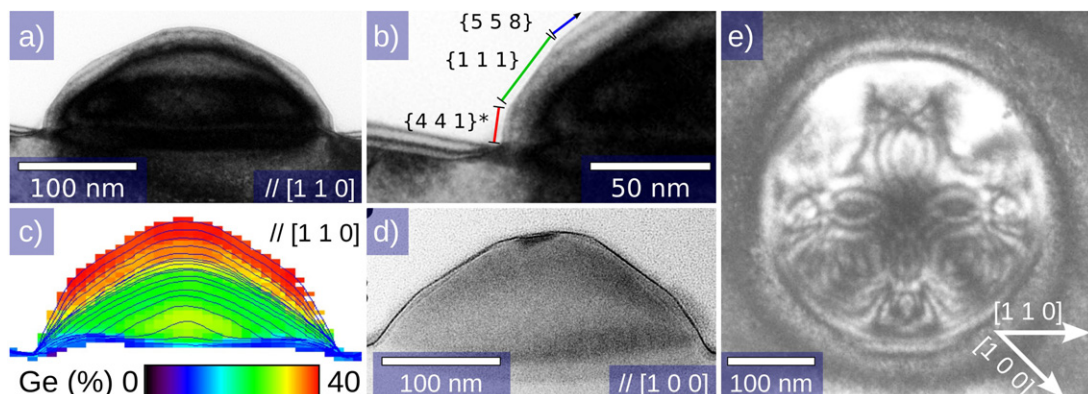

Figure 6. Panels (a) and (b) show TEM images of the 38 ML Ge sample along the [1 1 0] direction at different magnifications, with the steep surfaces highlighted in panel (b). Their inclination angle is about 80° with respect to the (0 0 1) surface. (c) Ge profile obtained by selective wet etching and AFM scans is shown, the steep facets cannot be assessed via conventional AFM due to the geometry of the AFM tip. In panel (d) a TEM image oriented along the [1 0 0] direction is shown. The contrast seen at the island apex is a result of damage during sample preparation. Image (e) features a plane-view TEM image of a cupola island. The symmetry of the strain contrast pattern, which also shows no splitting effects, confirms the absence of dislocations.
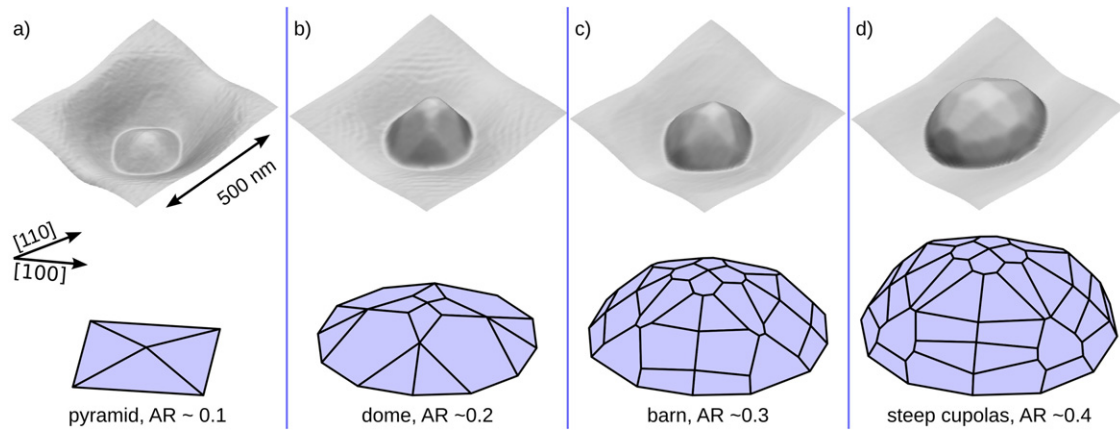
Figure 7. AFM data and sketches of the SiGe island shapes with (a) pyramids, (b) domes, (c) barns and the newly found steep cupolas (d).
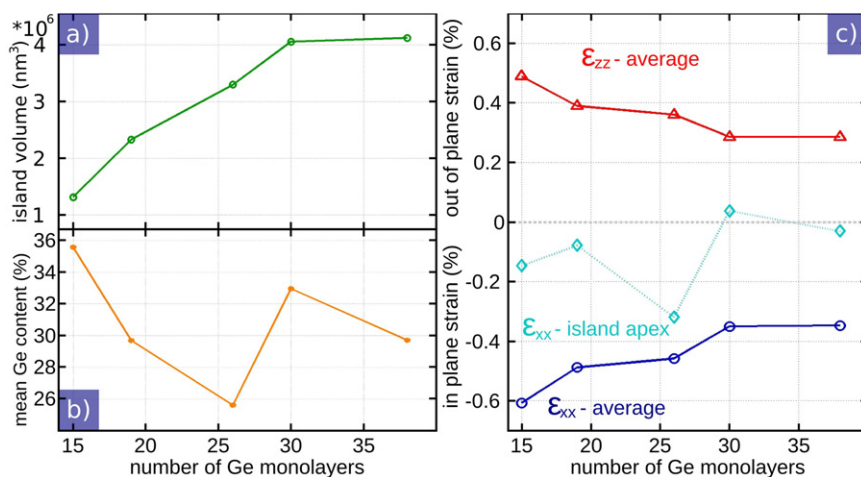

Figure 8. Simulation results in dependence of the Ge coverage (in ML): in panel (a) the island volume is displayed. Below, in section (b), the average Ge content, which displays a cyclic behavior with increasing Ge coverage, is shown. On the right side (c), plots of the corresponding average in-plane and out-of-plane strains within the islands are displayed. Both in-plane and out-of-plane strain decrease steadily with an increasing amount of deposited Ge. For the in-plane strain, additional values are given, which were obtained by integrating over the topmost 10 nm of the island apex in the center of the island.

the result of changes in island shape and complex intermixing processes.

One application of SiGe islands is their use as defect-free stressors, e.g., of Si cap layers grown on top of them. For this purpose, the in-plane strain in the topmost part of the islands is relevant, rather than the average in-plane strain. The corresponding values are plotted in figure 8(c) (light blue). For the steep cupolas, $\varepsilon_{xx} = 0.04\%$ is reached; with respect to the Si bulk lattice this value corresponds to a tensile strain of 1.8%.

In conclusion, we presented detailed investigations on the evolution of strain on SiGe islands obtained by depositing up to 38 ML of Ge on prepatterned Si(001) substrates. AFM and TEM investigations were used to examine the morphology of the samples and the occurrence of defects. As a main result of this paper, we find that SiGe islands with average contents in the 30% range can be fabricated defect-free and in a high density despite the large Ge coverage. Their shape changes in an oscillatory fashion with ongoing deposition. A new island shape with a higher aspect ratio than barns and with

ultra-steep facet sets was found (see figure 7), which means that the so far established growth-sequence is not 'the end of the story'.

Synchrotron-based XRD measurements of excellent quality provided both the input and fit parameter for strain calculations based on the finite element method. Those calculations, corroborated also by selective etching experiments, led us to another significant conclusion of this work: behind the pronounced changes in island shape and Ge distribution, a self-organized mechanism in order to relieve strain is in operation. In contrast to the shape and Ge content oscillations, both in-plane and out-of-plane strain values show a steady trend of increasing relaxation with higher Ge coverage. Hence different mechanisms such as lateral growth and Si uptake, as well as vertical growth and elastic relaxation, seem to share the same driving force, namely a reduction of the overall strain of the islands. To maintain coherent growth, it seems crucial that Ge is already incorporated into the pits and hence the islands grow on a 'prerelaxed' support.

This concept based on prepatterned substrates is certainly not limited to the SiGe system, but applicable also to other materials where islands form in the Stranski–Krastanov mode.

Acknowledgments

References

[1] Sun Y, Thompson S E and Nishida T 2010 *Strain Effect in Semiconductors—Theory and Device Applications* (New York: Springer) see also Journal of Applied Physics 101, 2007 (104503)

[2] Aqua J-N, Berbezier I, Favre L, Frisch T and Ronda A 2013 Growth and self-organization of SiGe nanostructures *Phys. Rep.* **522** 59–189

[3] Deneke C, Malachias A, Rastelli A, Merces L, Huang M H, Cavallo F, Schmidt O G and Lagally M G 2012 Straining nanomembranes via highly mismatched heteroepitaxial growth: in As islands on compliant Si substrates *ACS Nano* **6** 10287–95

[4] Huang M *et al* 2009 Mechano-electronic superlattices in silicon nanoribbons *ACS Nano* **3** 721–7

[5] Schliwa A, Winkelnkemper M and Bimberg D 2009 Few-particle energies versus geometry and composition of $In_xGa_{1-x}As$/GaAs self-organized quantum dots *Phys. Rev. B* **79** 075443

[6] Brehm M, Suzuki T, Fromherz T, Zhong Z, Hrauda N, Hackl F, Stangl J, Schaeffler F and Bauer G 2009 Combined structural and photoluminescence study of SiGe islands on Si substrates: comparison with realistic energy level calculations *New J. Phys.* **11** 063021

[7] Jovanov V, Eissfeller T, Kapfinger S, Clark E C, Klotz F, Bichler M, Keizer J G, Koenraad P M, Abstreiter G and Finley J J 2011 Observation and explanation of strong electrically tunable exciton *g* factors in composition engineered In(Ga)As quantum dots *Phys. Rev. B* **83** 161303

[8] Klenovsky P, Brehm M, Krapek V, Lausecker E, Munzar D, Hackl F, Steiner H, Fromherz T, Bauer G and Humlicek J 2012 Excitation intensity dependence of photoluminescence spectra of SiGe quantum dots grown on prepatterned Si substrates: evidence for biexcitonic transition *Phys. Rev. B* **86** 115305

[9] Schäffler F 1997 High-mobility Si and Ge structures *Semicond. Sci. Technol.* **12** 1515–49 and references therein

[10] Evans P G, Savage D E, Prance J R, Simmons C B, Lagally M G, Coppersmith S N, Eriksson M A and Schuelli T U 2012 Nanoscale distortions of Si quantum wells in Si/SiGe quantum-electronic heterostructures *Adv. Mater.* **24** 5217–21

[11] Eaglesham D J and Cerullo M 1990 Dislocation-free Stranski–Krastanow growth of Ge on Si(100) *Phys. Rev. Lett.* **64** 1943–6

[12] Mo Y W, Savage D E, Swartzentruber B S and Lagally M G 1990 Kinetic pathway in Stranski–Krastanov growth of Ge on Si(001) *Phys. Rev. Lett.* **65** 1020–3

[13] Stangl J, Holy V and Bauer G 2004 Structural properties of self-organized semiconductor nanostructures *Rev. Mod. Phys.* **76** 725–83

[14] Schmidt O G 2007 *Lateral Alignment of Epitaxial Quantum Dots* (Berlin: Springer)

[15] Miglio L and Montalenti F 2011 *Silicon–Germanium (SiGe) Nanostructures: Production, Properties, and Applications in Electronics* (Cambridge: Woodhead) chapter 10, p 656

[16] Schmidt O G and Eberl K 2001 Self-assembled Ge/Si dots for faster field-effect transistors *IEEE Trans. Electron Devices* **48** 1175

[17] Kar G S, Kiravittaya S, Denker U, Nguyen B Y and Schmidt O G 2006 Strain distribution in a transistor using self-assembled SiGe islands in source and drain regions *Appl. Phys. Lett.* **88** 253108

[18] Katsaros G, Spathis P, Stoffel M, Fournel F, Mongillo M, Bouchiat V, Lefloch F, Rastelli A, Schmidt O G and De Franceschi S 2010 Hybrid superconductor–semiconductor devices made from self-assembled SiGe nanocrystals on silicon *Nature Nanotechnol.* **5** 458–64

[19] Jovanović V *et al* 2010 *n*-channel MOSFETs fabricated on SiGe dots for strain-enhanced mobility *IEEE Electron Device Lett.* **31** 1083–5

[20] Hrauda N *et al* 2011 X-ray nanodiffraction on a single SiGe quantum dot inside a functioning field-effect transistor *Nano Lett.* **11** 2875–80

[21] Kratzer M, Rubezhanska M, Prehal C, Beinik I, Kondratenko S V, Kozyrev Yu N and Teichert C 2012 Electrical and photovoltaic properties of self-assembled Ge nanodomes on Si(001) *Phys. Rev. B* **86** 245320

[22] Ross F M, Tromp R M and Reuter M C 1999 Transition states between pyramids and domes during Ge/Si island growth *Science* **286** 1931–4

[23] Katsaros G, Costantini G, Stoffel M, Esteban R, Bittner A M, Rastelli A, Denker U, Schmidt O G and Kern K 2005 Kinetic origin of island intermixing during the growth of Ge on Si(001) *Phys. Rev. B* **72** 195320

[24] Zhang J J, Stoffel M, Rastelli A, Schmidt O G, Jovanović V, Nanver L K and Bauer G 2007 SiGe growth on patterned Si(001) substrates: surface evolution and evidence of modified island coarsening *Appl. Phys. Lett.* **91** 173115

[25] Zhong Z, Schwinger W, Schäffler F, Bauer G, Vastola G, Montalenti F and Miglio L 2007 Delayed plastic relaxation on patterned Si substrates: coherent SiGe pyramids with dominant {1 1 1} facets *Phys. Rev. Lett.* **98** 176102

[26] Brehm M *et al* 2009 Key role of the wetting layer in revealing the hidden path of Ge/Si(001) Stranski–Krastanow growth onset *Phys. Rev. B* **80** 205321

[27] Vailionis A, Cho B, Glass G, Desjardins P, Cahill D G and Greene J E 2000 Pathway for the strain-driven two-dimensional to three-dimensional transition during growth of Ge on Si(001) *Phys. Rev. Lett.* **85** 3672–5

[28] Rastelli A, Von Känel H, Spencer B J and Tersoff J 2003 Prepyramid-to-pyramid transition of SiGe islands on Si(001) *Phys. Rev. B* **68** 115301

[29] Medeiros-Ribeiro G, Bratkovski A M, Kamins T I, Ohlberg D A A and Williams R S 1998 Shape transition of germanium nanocrystals on a silicon(001) surface from pyramids to domes *Science* **279** 353–5

[30] Sutter E, Sutter P and Bernard J E 2004 Extended shape evolution of low mismatch $Si_{1-x}Ge_x$ alloy islands on Si(100) *Appl. Phys. Lett.* **84** 2262–4

[31] Rastelli A, Stoffel M, Denker U, Merdzhanova T and Schmidt O G 2006 Strained SiGe islands on Si(001): evolution, motion, dissolution, and plastic relaxation *Phys. Status Solidi* a **203** 3506–11

[32] Stoffel M, Rastelli A, Tersoff J, Merdzhanova T and Schmidt O G 2006 Local equilibrium and global relaxation of strained SiGe/Si(001) layers *Phys. Rev. B* **74** 155326

[33] LeGoues F K, Reuter M C, Tersoff J, Hammar M and Tromp R M 1994 Cyclic growth of strain-relaxed islands *Phys. Rev. Lett.* **73** 300–3

[34] Merdzhanova T, Kiravittaya S, Rastelli A, Stoffel M, Denker U and Schmidt O G 2006 Dendrochronology of strain-relaxed islands *Phys. Rev. Lett.* **96** 226103

[35] Brehm M, Lichtenberger H, Fromherz T and Springholz G 2011 Ultra-steep side facets in multi-faceted SiGe/Si(001) Stranski–Krastanow islands *Nanoscale Res. Lett.* **6** 70

[36] Zhang J J *et al* 2010 Collective shape oscillations of SiGe islands on pit-patterned Si(001) substrates: a coherent-growth strategy enabled by self-regulated intermixing *Phys. Rev. Lett.* **105** 166102

[37] Rastelli A, Stoffel M, Malachias A, Merdzhanova T, Katsaros G, Kern K, Metzger T H and Schmidt O G 2008 Three-dimensional composition profiles of single quantum dots determined by scanning-probe-microscopy-based nanotomography *Nano Lett.* **8** 1404–9

[38] Stoffel M, Malachias A, Merdzhanova T, Cavallo F, Isella G, Chrastina D, von Kanel H, Rastelli A and Schmidt O G 2008 SiGe wet chemical etchants with high compositional selectivity and low strain sensitivity *Semicond. Sci. Technol.* **23** 085021

[39] Carns T K, Tanner M O and Wang K L 1995 Chemical etching of $Si_{1-x}Ge_x$ in Hf–H_2O_2–CH_3COOH *J. Electrochem. Soc.* **142** 1260–6

[40] Seeck O H *et al* 2012 The high-resolution diffraction beamline P08 at PETRA III *J. Synchrotron Radiat.* **19** 30–8

[41] http://pilatus.web.psi.ch/mythen.htm *Mythen Position Sensitive Detector*

[42] www.comsol.com/ *COMSOL Multiphysics Package*

[43] Pietsch U, Holý V and Baumbach T 2004 *High-Resolution X-Ray Scattering from Thin Films and Multilayers* 2nd edn (Berlin: Springer)

[44] Schmidbauer M 2004 *X-Ray Diffuse Scattering from Self-Organized Mesoscopic Semiconductor Structures* (*Springer Tracts in Modern Physics* vol 199) (Berlin Heidelberg: Springer)

[45] Bergamaschini R, Tersoff J, Tu Y, Zhang J J, Bauer G and Montalenti F 2012 Anomalous smoothing preceding island formation during growth on patterned substrates *Phys. Rev. Lett.* **109** 156101

[46] Chen G, Lichtenberger H, Bauer G, Jantsch W and Schäffler F 2006 Initial stage of the two-dimensional to three-dimensional transition of a strained SiGe layer on a pit-patterned Si(001) template *Phys. Rev.* B **74** 035302

[47] Gai Z, Yang W S, Zhao R G and Sakurai T 1999 Macroscopic and nanoscale faceting of germanium surfaces *Phys. Rev.* B **59** 15230–9 and references therein

[48] Robinson J T, Rastelli A, Schmidt O and Dubon O D 2009 Global faceting behavior of strained Ge islands on Si *Nanotechnology* **20** 085708

[49] Boioli F, Gatti R, Grydlik M, Brehm M, Montalenti F and Miglio L 2011 Assessing the delay of plastic relaxation onset in SiGe islands grown on pit-patterned Si(001) substrates *Appl. Phys. Lett.* **99** 033106

[50] Schülli T U *et al* 2009 Enhanced relaxation and intermixing in Ge islands grown on pit-patterned Si(001) substrates *Phys. Rev. Lett.* **102** 025502